Congenital Heart Disease

Tech Science Press

DOI: 10.32604/chd.2022.020401

ARTICLE

Comparison of Intracardiac and Extracardiac Malformations Associated with Single Atrium, Single Ventricle and Single Atrium-Single Ventricle Using Dual-Source Computed Tomography

Tong Pang[#], Li Jiang[#], Yi Zhang, Mengxi Yang, Jin Wang, Yuan Li[*] and Zhigang Yang[*]

Department of Radiology, West China Hospital, Sichuan University, Chengdu, 610041, China

[*]Corresponding Authors: Zhigang Yang. Email: yangzg666@163.com; Yuan Li. Email: dr.liyuan@163.com

[#]These authors equally contributed to this work as first author

Received: 22 December 2021 Accepted: 10 March 2022

ABSTRACT

Background: To evaluate the qualitative and quantitative differences between intracardiac and extracardiac vascular malformations in patients with a single atrium (SA), single ventricle (SV) and single atrium-single ventricle (SA-SV) using dual-source CT (DSCT), and to compare the diagnostic performances of DSCT and transthoracic echocardiography (TTE). **Methods:** This retrospective study included 24 SA, 75 SV and 24 SA-SV patients who underwent both DSCT and TTE before surgery. The diagnostic values of DSCT and TTE for intracardiac and extracardiac malformations were compared according to the surgical results. The diameters of the major artery and vein were measured and calculated based on DSCT and compared among the three groups. **Results:** The most common malformation was pulmonary artery disease in SA (50.0%) and SA-SV (45.8%) groups and patent ductus arteriosus (33.3%) in SV group. Although there was no statistical difference, arterial development was relatively poor in the SA group. All groups showed the trend of pulmonary artery stenosis (SA *vs.* SV *vs.* SA-SV: 50.0% *vs.* 30.7% *vs.* 33.3%). There was a significant difference in mean pulmonary vein index among the groups ($p = 0.017$). The diagnostic sensitivity of DSCT was superior to that of TTE for extracardiac malformations. **Conclusions:** The most common malformation in SA and SA-SV patients is pulmonary artery stenosis. SV patients are most likely to be complicated with patent ductus arteriosus. DSCT is more advantageous than TTE for diagnosing combined extracardiac malformations and can accurately measure the diameter of arteriovenous vessels.

KEYWORDS

Single atrium; single ventricle; computed tomography; congenital heart disease

1 Introduction

Single atrium (SA), single ventricle (SV) and single atrium-single ventricle (SA-SV) are all rare cyanotic congenital heart diseases caused by embryonic dysplasia of the atrium or ventricle. SA is caused by an undeveloped first and second septum of the atrial septum during embryonic development [1–3]. SV is also known as ventricular double entrance or single ventricular atrioventricular connection [4,5]. SA-SV, which refers to an individual with both of the above diseases, is very rare [6].

They are often complicated with other intracardiac and extracardiac malformations that require surgery or intervention. The anatomy and 3D structure of the great mediastinal vessels and their degree of

development significantly influence the choice of surgical methods [2,5]. In clinical practice, the McGoon ratio, pulmonary artery index (PAI), total new pulmonary artery index (TNPAI) and pulmonary vein index (PVI) are often used for patient evaluations to help formulate the surgical plan [7,8]. Therefore, imaging data is crucial to obtain an accurate preoperative evaluation of patients with SA, SV or SA-SV.

Dual-source CT (DSCT) has been widely used to evaluate complex congenital heart disease [9] and has been shown to accurately evaluate morphologic changes in the heart and vessels of patients with congenital heart disease before and after surgery [2,5,10–15]. However, there are few reports of the qualitative and quantitative evaluation of DSCT in a large number of patients with SA, SV or SA-SV. As a national centre for the diagnosis and treatment of complex and severe diseases in Western China, we are able to collect data on a relatively large number of patients with SA, SV or SA-SV. Therefore, this study aims to evaluate the qualitative and quantitative differences between intracardiac and extracardiac vascular malformations in patients with SA, SV or SA-SV using DSCT based on this relatively large cohort. It will also compare the diagnostic performance between DSCT and transthoracic echocardiography (TTE).

2 Materials and Methods

2.1 Patients

A total of 138 patients with SA, SV or SA-SV confirmed by surgery from October 2008 to April 2021 were included. They all underwent enhanced DSCT and TTE scans at our hospital. We excluded patients with incomplete crucial clinical data or imaging data that could not be analysed. The final cohort comprised 123 patients. All relevant intracardiac and extracardiac abnormalities and their percentages were recorded.

This study was approved by the Biomedical Research Ethics Committee of West China Hospital, Sichuan University (No. 14-163). Patient consent was waived due to the retrospective nature of this investigation.

2.2 Dual-Source Computed Tomography

All scans were performed using a DSCT scanner (SOMATON Definition Flash; Siemens Medical Solutions, Forchheim, Germany). Prior to examination, patients younger than 6-years-old were administered short-acting sedatives (10% chloral hydrate at a concentration, 0.5 ml/kg). The acquisition parameters of the ECG-gated protocol were as follows: tube voltage, 80 kV; tube current, 100 mAs; gantry rotation time, 0.28 s and pitch, 0.2–0.5 (selected according to the heart rate; the pitch was positively correlated with heart rate). The ECG-pulsing window was set on auto. The scanning range was from the thoracic entrance to 2 cm below the diaphragm, in the posterior direction. During angiography, a non-ionic contrast medium (iopamidol, 370 mg/ml) was injected through the anterior cubital fossa at a speed of 1.2–2.5 ml/s, and then 20 ml of normal saline was injected at the same flow rate. The injection volume was adjusted for body weight (1.5 ml/kg). Using 100 HU as the predefined threshold, bolus tracking was performed in the region of interest (ROI) of the descending aorta. When the ROI attenuation threshold reaches 100 HU, image acquisition is triggered after a 5 s delay. The data were processed at a Syngo workstation (Siemens Medical Systems, Forchheim, Germany). The images were reconstructed at a slice thickness of 0.75 mm and in increments of 0.7 mm.

2.3 Transthoracic Echocardiography

All patients underwent the TTE examination that included M-mode, 2D, continuous-wave and colour Doppler flow imaging with a Philips SONOS 7500 ultrasound system (Philips Medical Systems, Bothell, WA), according to the recommendations of the committee of the American Society of Echocardiography [16]. The interval between DSCT and TTE was <14 days.

2.4 Data Measurement and Analysis

DSCT images were reconstructed into 3D images that were used to measure the diameter and area of the pulmonary artery and vein. The diameter of the descending aorta was measured at the level of the diaphragm (Fig. 1A), and those of the superior and inferior vena cava were measured at the level of the atrium (Figs. 1E and 1F) [17]. The diameters of the pulmonary artery and the pulmonary vein were measured in the sagittal or coronal view. The diameter of the pulmonary trunk was measured at the level of pulmonary bifurcation (Fig. 1D). The left and right pulmonary arterial diameters were measured at 1 cm distal to the bifurcation of the left and right pulmonary arteries (Figs. 1A and 1B). The collateral vessels >2 mm in diameter were measured at the proximal orifices [18]. The diameter of each pulmonary vein before the atrium entrance was also measured (Fig. 1C). The cross-sectional area of each pulmonary vein was calculated assuming that it was round [8,19], the McGoon ratio, PAI, TNPAI and PVI were calculated by the following formula [8,19]:

$$\text{McGoon} = \frac{\text{the diameters of (left pulmonary artery + right pulmonary artery)}}{\text{the diameter of the aorta at diaphragm level}}$$

$$\text{PAI} = \frac{\text{the cross sectional areas of (left pulmonary artery + right pulmonary artery)}}{\text{the body surface area}}$$

$$\text{TNPAI} = \frac{\text{the cross sectional areas of (left pulmonary artery + right pulmonary artery + collateral vessel)}}{\text{the body surface area}}$$

$$\text{PVI} = \frac{\text{the total cross sectional areas of four pulmonary veins}}{\text{the body surface area}}$$

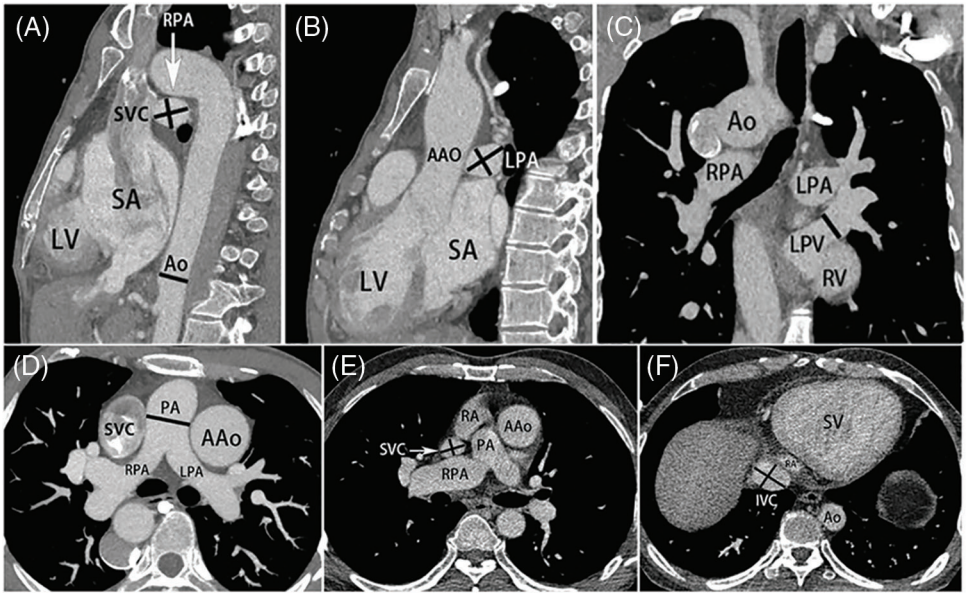

Figure 1: Measurement diagram. (A) The diameter of the DAo was measured at the level of the diaphragm. (B, C) The diameters of the pulmonary artery and pulmonary vein were measured in the sagittal or coronal view. The left and right pulmonary arterial diameters were measured at 1 cm distal to the bifurcation of the left and right pulmonary arteries. (D) The diameter of the pulmonary trunk was measured at the level of pulmonary bifurcation. (E, F) The diameters of the SVC and IVC were measured at the level of the atrium. SA = single atrium, LV = left ventricle, Ao = aortic, SVC = superior vena cava, RPA = right pulmonary artery, AAo = ascending aorta, DAo = descending aorta, LPA = left pulmonary artery, LPV = left pulmonary vein, RV = right ventricle, PA = pulmonary artery, RA = right atrium, SV = single ventricle, IVC = Inferior vena cava

The normal McGoon ratio is >2.0 and the normal PAI value is 330 ± 30 mm^2/m^2 [15]. If the McGoon ratio is >1.2 and PAI > 150 mm^2/m^2, one-stage radical surgery can be considered [20–23]. Patients with TNPAI > 200 mm^2/m^2 can safely undergo ventricular septal defect repair, whereas patients with TNPAI < 150 mm^2/m^2 can only undergo right ventricular outflow tract reconstruction in stage 1 [24,25].

2.5 Statistical Analysis

The data were analysed using SPSS software v22.0 (IBM Corp, Armonk, NY). The Shapiro–Wilk test was performed to confirm the normality of the distribution of continuous variables. Normally distributed continuous variables were expressed as mean ± standard deviations and tested by one-way analysis of variance among the SA, SV and SA-SV groups. Categorical variables were expressed as numbers and percentages and tested using the Fisher exact test or chi-square test, as appropriate. The results of surgical findings were utilised as the reference standard. The sensitivity, specificity and positive and negative predictive values were calculated for separate cardiovascular anomalies. The accuracy of DSCT and TTE was compared using the chi-square test. A p-value < 0.05 was considered statistically significant.

3 Results

3.1 Baseline Characteristics

Of the 123 patients in our cohort, 24 had SA, 75 had SV and 24 had SA-SV. There was no statistical difference in sex (male, SA *vs*. SV *vs*. SA-SV, 13 [54.20%] *vs*. 44 [58.70%] *vs*. 12 [50.00%]; $p = 0.698$), age (SA *vs*. SV *vs*. SA-SV, 4.4 ± 4.0 years *vs*. 7.6 ± 6.9 years *vs*. 6.8 ± 6.2 years; $p = 0.101$) and body mass index (SA *vs*. SV *vs*. SA-SV, 15.7 ± 1.6 kg/m^2 *vs*. 14.9 ± 2.3 kg/m^2 *vs*. 14.1 ± 2.7 kg/m^2; $p = 0.054$) among the three groups.

The oxygen saturation level was significantly decreased among the three groups. The SA-SV group showed a statistically significant and higher blood oxygen saturation level than the SA and SV groups (SA *vs*. SV *vs*. SA-SV, 89.0% ± 5.1% *vs*. 87.4% ± 4.9% *vs*. 91.5 ± 4.3%; $p = 0.046$). The most common symptoms in the SA and SA-SV patients were heart murmurs (SA, 18/24, 75.0% and SA-SV, 21/24, 87.5%) and cyanosis (53/75, 70.7%) was the most common in SV patients (Table 1).

Table 1: Baseline patient characteristics

	SA (n = 24)	SV (n = 75)	SA-SV (n = 24)	*P*
Sex (Male)	13 (54.2%)	44 (58.7%)	12 (50.0%)	0.698
Age, years	4.4 ± 4.0	7.6 ± 6.9	6.8 ± 6.2	0.101
Height, cm	98.7 ± 26.3	100.7 ± 30.3	95.3 ± 32.7	0.743
Weight, kg	9.9 ± 5.8	12.1 ± 8.6	11.7 ± 7.4	0.670
Body mass index, kg/m^2	15.7 ± 1.6	14.9 ± 2.3	14.1 ± 2.7	0.054
Heart rate, bpm	127.5 ± 15.8	116.6 ± 22.9	120.4 ± 12.4	0.069
Systolic blood pressure, mmHg	90.1 ± 16.7	85.4 ± 18.8	93.6 ± 24.4	0.175
Diastolic blood pressure, mmHg	55.9 ± 14.3	63.6 ± 13.1	60.8 ± 18.7	0.075
Oxygen saturation, %	89.0 ± 5.1	87.4 ± 4.9*	91.5 ± 4.3*	0.046
Symptoms				
Heart murmurs	18 (75.0%)	48 (64.0%)	21 (87.5%)	0.460
Cyanosis	13 (54.2%)	53 (70.7%)	17 (70.8%)	0.136
Squatting	9 (37.5%)	30 (40.0%)	8 (33.3%)	0.827
Post-exercising tachypnea	10 (41.7%)	31 (48.0%)	9 (37.5%)	0.588

Abbreviations: SA, single atrium; SV, single ventricle; SA-SV, single atrium-single ventricle; *, p-value < 0.05.

3.2 Comparison of Intracardiac and Extracardiac Malformations among Three Groups

The various intracardiac and extracardiac malformations observed during surgery are detailed in Table 2. In terms of intracardiac malformation, patients with SV are most likely to be associated with atrial septal defect (33/75, 44.0%). In patients with SA, the most common abnormalities were pulmonary artery stenosis (12/24, 50.0%) and pulmonary valve stenosis (10/24, 41.7%) (Fig. 2). In SV patients, the top three malformations were patent ductus arteriosus (25/75, 33.3%), pulmonary artery stenosis (23/75, 30.7%) and right ventricular double outlet (20/75, 26.7%) (Fig. 3). In the patients with SA-SV, the incidence of pulmonary artery dilation (11/24, 45.8%), right aortic arch (10/24, 41.7%), right ventricular outflow tract stenosis (9/24, 37.5%), coarctation of aorta (9/24, 37.5%) were more pronounced (Fig. 4).

Table 2: Intracardiac and extracardiac malformations in patients with SA, SV and SA-SV

Intracardiac and extracardiac malformations	SA (n = 24)	SV (n = 75)	SA-SV (n = 24)	*P*
Extracardiac malformations	**76**	**171**	**93**	
PLSVC	7 (29.2%)	16 (21.3%)	7 (29.2%)	0.429
Partial anomalous pulmonary venous connection	2 (8.3%)	5 (6.6%)	3 (12.5%)	0.546
Total anomalous pulmonary venous connection	3 (12.5%)	9 (12.0%)	6 (25.0%)	0.223
Double superior vena cava	5 (20.8%)	15 (20.0%)	7 (29.2%)	0.347
Right-sided aortic arch	6 (25.0%)	13 (17.3%) *	10 (41.7%) *	0.024
Double aortic arch	1 (4.2%)	4 (5.3%)	1 (4.2%)	0.658
Bicuspid aortic valve	2 (8.3%)	4 (5.3%)	2 (8.3%)	0.964
Supravalvular aortic stenosis	5 (20.8%)	8 (10.7%)	4 (16.7%)	0.349
Coarctation of aorta	6 (25.0%) †	3 (4.0%) †§	9 (37.5%) §	0.009
Pulmonary atresia	3 (12.5%)	9 (12.0%)	7 (29.2%)	0.095
Pulmonary artery stenosis	12 (50.0%)	23 (30.7%)	8 (33.3%)	0.085
Pulmonary artery dilation	2 (8.3%) §	5 (6.6%) †	11 (45.8%) †§	0.004
Pulmonary valve stenosis	10 (41.7%)	13 (17.3%)	5 (20.8%)	0.320
Absent pulmonary valve syndrome	0 (0%)	1 (1.3%)	1 (4.2%)	0.534
Anomalous origin of pulmonary artery	1 (4.2%)	4 (5.3%)	2 (8.3%)	0.964
Patent ductus arteriosus	7 (29.2%)	25 (33.3%)	6 (25.0%)	0.445
Aortopulmonary collateral vessels	2 (8.3%)	4 (5.3%)	3 (12.5%)	0.566
Coronary artery anomalies	2 (8.3%)	10 (13.3%)	1 (4.1%)	0.384
Intracardiac malformations	**18**	**70**	**18**	
ASD	–	33 (44.0%)	–	–
VSD	6 (25.0%)	–	–	–
Double outlet right ventricle	6 (25.0%)	20 (26.7%)	8 (33.3%)	0.525
Right ventricular outflow tract stenosis	5 (20.8%)	14 (18.7%)	9 (37.5%)	0.157
Left ventricular outflow tract stenosis	1 (4.2%)	3 (4.0%)	1 (4.2%)	0.758
Total	**94**	**241**	**111**	

Abbreviations: SA, single atrium; SV, single ventricle; SA-SV, single atrium-single ventricle; PLSVC, persistent left superior vena cava; ASD, atrial spetal defect; VSD, ventricular septal defect; *, p-value < 0.05; † §, p value < 0.01.

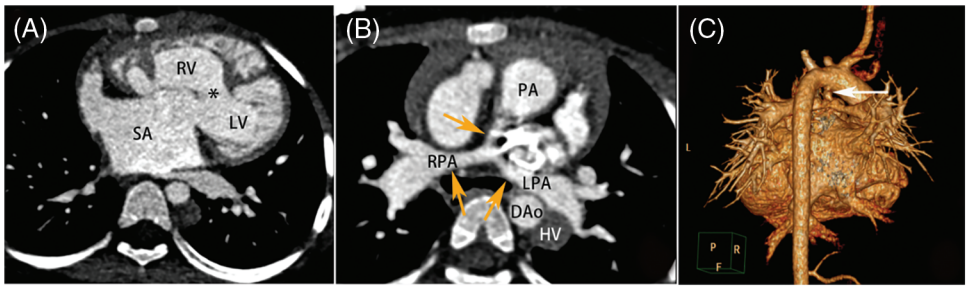

Figure 2: SA in a female aged 4 years. (A) The transverse plane of a SA with a ventricular septal defect (*). (B) Axial image shows the pulmonary trunk; LPA and RPA were stenosed (yellow arrow). The HV is thickened and located on the left side of DAo. (C) VR image shows the patent ductus arteriosus entering the PA from the Ao (white arrow). DAo = descending aorta, HV = hemiazygos vein, VR = volume rendering, other abbreviations as in Fig. 1

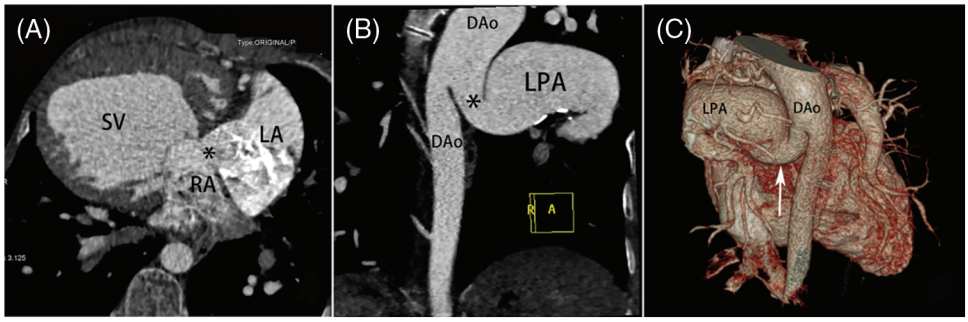

Figure 3: SV in a male aged 13 years. (A) The transverse plane of a SV with atrial septal defect (*) and dextrocardia. (B) (C) MPR and VR images show that the DAo communicates with the LPA (*) (white arrow). VR image shows that the left pulmonary artery sends out many small branches. LA = left atrium, MPR = multiple planar reconstruction, other abbreviations as in Figs. 1 and 2

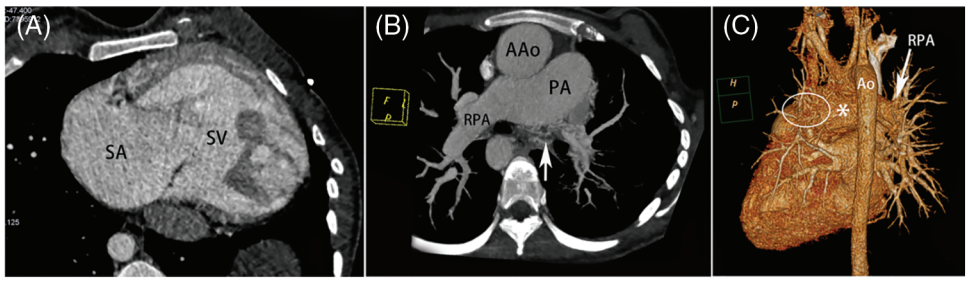

Figure 4: SA-SV in a female aged 9 years. (A) The transverse plane of a SA-SV. (B, C) The MPR and VR images show the absence of the left pulmonary artery (*) and multiple collateral circulation in the mediastinum (white arrow) (ellipse). SA-SV = single atrium-single ventricle, other abbreviations as in Figs. 1–3

We found 13 right-sided aortic arches in SV patients and 10 in SA-SV patients ($p < 0.05$). A total of three SV patients had coarctation of aorta, compared with six SA patients and nine SA-SV patients ($p < 0.01$). Pulmonary artery dilatation occurred in 11 SA-SV patients, compared with two SA patients and five SV patients ($p < 0.01$). The incidence of both intracardiac and extracardiac malformations was higher in patients with SA-SV than in those with SA or SV.

3.3 Comparison of the Measurement and Calculation Results of the Major Arteries and Veins

The McGoon ratio, PAI, TNPAI and PVI were measured by DSCT and compared among patients with SA, SV or SA-SV (Table 3). The McGoon ratio, PAI and TNPAI were lower in SA group than in other groups (McGoon ratio < 1.2, 20 [83.3%]; PAI < 150 mm^2/m^2, 19 [79.2%]; TNPAI < 200 mm^2/m^2, 20 [83.3%]). There was a significant difference in mean PVI among the three groups (SA *vs*. SV *vs*. SA-SV, 150.49 ± 75.18 mm^2/m^2 *vs*. 214.84 ± 127.82 mm^2/m^2 *vs*. 107.01 ± 53.41 mm^2/m^2; $p = 0.017$). Although the difference in arterial-related data among the three groups was not statistically significant, they all showed a trend of pulmonary artery stenosis or pulmonary atresia (McGoon ratio:SA *vs*. SV *vs*. SA-SV, 0.92 ± 0.42 *vs*. 0.97 ± 0.33 *vs*. 1.05 ± 0.47; $p = 0.753$).

Table 3: DSCT measurements of the major arteries and veins

	SA (n = 24)	SV (n = 75)	SA-SV (n = 24)	*p*
Pulmonary trunk, cm	1.45 ± 0.60	1.18 ± 0.90	1.35 ± 0.92	0.647
Left pulmonary artery, cm	1.01 ± 0.30	1.26 ± 0.76	0.79 ± 0.40	0.071
Right pulmonary artery, cm	0.99 ± 0.35	1.16 ± 0.67	1.09 ± 0.37	0.473
Collateral vessel, cm	0.46 ± 0.23	0.63 ± 0.48	0.51 ± 0.35	0.621
Descending aorta at diaphragm level, cm	2.37 ± 0.86	2.04 ± 0.83	2.56 ± 0.82	0.354
Superior vena cava, cm	1.62 ± 0.96	1.99 ± 0.65	1.53 ± 0.41	0.211
Inferior vena cava, cm	2.23 ± 0.70	2.12 ± 1.19	1.89 ± 0.92	0.696
McGoon ratio	0.92 ± 0.42	0.97 ± 0.33	1.05 ± 0.47	0.753
McGoon < 1.2	20 (83.3%)	51 (68.0%)	18 (75.0%)	0.147
PAI (mm^2/m^2)	127.81 ± 93.87	143.77 ± 107.24	131.44 ± 99.90	0.341
PAI < 150	19 (79.2%)	48 (64.0%)	16 (66.7%)	0.167
TNPAI (mm^2/m^2)	151.53 ± 101.64	172.69 ± 118.66	160.57 ± 113.11	0.504
TNPAI < 200	20 (83.3%)	47 (62.7%)	16 (66.7%)	0.060
PVI (mm^2/m^2)	150.49 ± 75.18*	214.84 ± 127.82*§	107.01 ± 53.41§	0.017

Abbreviations: SA, single atrium; SV, single ventricle; SA-SV, single atrium-single ventricle; PAI, pulmonary artery index; TNPAI, total new pulmonary artery index; PVI, pulmonary vein index; *, *p*-value < 0.05. §, *p*-value < 0.01.

3.4 Comparison of Diagnostic Accuracy between DSCT and TTE

DSCT was similar to TTE in terms of extracardiac malformation, but TTE had a smaller advantage (DSCT *vs.* TTE: sensitivity, 94.1% *vs*. 88.2% in SA; 95.6% *vs*. 93.3% in SV and 100.0% *vs*. 92.0% in SA-SV). However, DSCT was slightly insufficient compared with TTE in terms of intracardiac malformations (DSCT *vs*. TTE: sensitivity, 100.0% *vs*. 100.0% in SA; 91.9% *vs*. 100.0% in SV and 93.8% *vs*. 96.2% in SA-SV) (Table 4).

4 Discussion

We used DSCT to qualitatively analyse the intracardiac and extracardiac vascular malformations of patients with SA, SV and SA-SV, respectively, and to quantitatively measure the diameter or surface area of the vascular lumen in the three groups. We further compared the diagnostic consistency of DSCT with TTE in intracardiac and intracardiac vascular malformations. The main findings of this study are as follows: (1) The incidence rate of intracardiac and extracardiac malformations differed in patients with SA, SV and SA-SV. (2) The McGoon ratio of patients with SA, SV and SA-SV showed a trend of pulmonary stenosis, while the PVI of these patients was significantly different. (3) The diagnostic performance of DSCT was superior to that of TTE for extracardiac vascular malformations.

Table 4: The diagnostic accuracy of DSCT and TTE in patients with SA, SV and SA-SV

Anomalies categories	DSCT				TTE			
	Sensitivity	**Specificity**	**PPV**	**NPV**	**Sensitivity**	**Specificity**	**PPV**	**NPV**
SA (n = 24)								
Extracardiac anomalies	94.1%	100.0%	100.0%	98.2%	88.2%	96.4%	88.2%	96.4%
Intracardiac anomalies	100.0%	99.1%	96.6%	100.0%	100.0%	99.1%	96.6%	100.0%
SV (n = 75)								
Extracardiac anomalies	95.6%	100.0%	100.0%	98.9%	93.3%	98.3%	93.3%	98.3%
Intracardiac anomalies	91.9%	100.0%	100.0%	98.4%	100.0%	100.0%	100.0%	100.0%
SA-SV (n = 24)								
Extracardiac anomalies	100.0%	100.0%	100.0%	100.0%	92.0%	98.9%	95.8%	97.9%
Intracardiac anomalies	93.8%	100.0%	100.0%	98.2%	96.2%	100.0%	100.0%	98.9%

Abbreviation: SA, single atrium; SV, single ventricle; SA-SV, single atrium-single ventricle; PPV, positive predictive value; NPV, negative predictive value.

The incidence of both intracardiac and extracardiac malformations is higher in patients with SA-SV than in those with SA or SV. Consistent with previous studies, pulmonary disease is one of the top three malformations in patients with SA, SV and SA-SV [20–22]. The McGoon ratio, PAI and TNPAI are generally used to evaluate the state of natural pulmonary artery development before surgery. Therefore, we measured the McGoon ratio, PAI and TNPAI to quantitatively evaluate the degree of development of the pulmonary artery. The normal McGoon ratio is >2.0 and the normal PAI value is 330 ± 30 mm^2/m^2 [17]. If the McGoon ratio is >1.2 and PAI > 150 mm^2/m^2, one-stage radical surgery can be considered [23–25]. The data measured in our study by reconstruction technology showed a mean McGoon ratio of <1.2 and a mean PAI of <150 mm^2/m^2 in all three groups, suggesting pulmonary artery dysplasia. In many cases, the source of pulmonary blood is complex and diverse, so the pulmonary circulation flow represented by the pulmonary artery may be deviated. Therefore, we measured TNPAI as a correction of PAI. Reddy et al. found that all patients with TNPAI > 200 mm^2/m^2 could safely undergo ventricular septal defect repair, while patients with TNPAI < 150 mm^2/m^2 could only undergo right ventricular outflow tract reconstruction in stage 1 [26,27]. Our data showed that the mean TNPAI in all three groups was <200 mm^2/m^2, suggesting that there is a high probability of failure to close the septal defect safely, especially in SA patients, which has a considerable impact on the choice of surgical methods. Such findings help in identifying majority of the patients unsuitable for undergoing radical surgery, thereby simplifying clinical work.

Some studies have suggested that the area of the pulmonary vein is more representative of pulmonary circulation flow than the area of the pulmonary artery, and PVI reflects the development of the pulmonary vascular bed better than PAI [28]. Thus, we also measured the pulmonary vein diameter and calculated PVI [29]. There were significant differences in PVI among the three groups, especially between patients with SA and SA-SV. SA is often associated with left superior vena cava and dextrocardia. These complicated malformations may change the mediastinal morphology, resulting in diameter stenosis of the pulmonary veins in front of the atrium entrance [30].

Our results showed that DSCT was superior to TTE in the diagnosis of extracardiac malformations. The small field of vision of the parasternal sound window may be the main reason why TTE cannot accurately identify large vessels compared with DSCT [31,32]. Abnormalities of main pulmonary collateral vessels and coronary arteries are often missed or misdiagnosed when using TTE, which may be because TTE can only identify relatively large vessels, whereas DSCT can display the number, source and shape of all main pulmonary collateral vessels, regardless of the vessel size [32]. However, in terms of intracardiac malformation, DSCT missed one case of pulmonary valve syndrome and bicuspid aortic valve in the SA-SV group, which was slightly inferior to TTE. This can be partly explained as due to image artefacts caused by motion or contrast agents or may be because it is difficult to use DSCT to evaluate small intracardiac malformations based on static 2D images.

For children receiving DSCT, the risk of radiation exposure remains a major concern, particularly in infancy, because children are at higher risk of DNA mutations [33,34]. Therefore, in this study DSCT scanning was conducted in strict accordance with the as low as reasonably achievable (ALARA) principle [35].

5 Limitations

There are several limitations of our study. Firstly, this is a retrospective single-centre study, so a more extensive multicentre study should be performed in the future to confirm the generalisability of our findings. Secondly, we did not conduct long-term follow-up of patients to determine postoperative characteristics and outcomes, and this may be discussed in future studies. Finally, children are exposed to radiation from DSCT, but effective measures have been taken to minimise radiation doses.

6 Conclusions

Patients with SA, SV or SA-SV were often complicated with multiple intracardiac and extracardiac malformations identified by DSCT, and pulmonary vascular anomalies was the most common malformation. DSCT has better diagnostic performance in the preoperative evaluation of extracardiac vascular malformations in patients with SA, SV or SA-SV than TTE, especially in the diagnosis of extracardiac malformations, such as pulmonary artery development and main pulmonary collateral vessels. It can accurately measure the diameter of arteriovenous vessels using 3D reconstruction techniques, thereby providing surgeons with more detailed morphologic pictures.

Authorship: PT designed the study and collected, sorted, statistical data and wrote the manuscript. JL participated in the study design, analyzed the data, drafted the manuscript and editing and review of the manuscript. ZY and YMX checked the quality of the image and classified, JY and WJ reviewed the classification results of them. YZG and LY supervised the overall study and contributed to study design, editing and review of the manuscript. All authors reviewed the results and approved the final version of the manuscript.

Availability of Data and Materials: The datasets used and analysed in the current study are available from the corresponding author on reasonable request.

Funding Statement: This work was supported by Sichuan Science and Technology Program [2020YJ0229] and 1·3·5 Project for Disciplines of Excellence, West China Hospital, Sichuan University [ZYGD18013].

Conflicts of Interest: The authors declare that they have no conflicts of interest to report regarding the present study.

References

1. Jiang, H., Wang, H., Wang, Z., Zhu, H., Zhang, R. (2013). Surgical correction of common atrium without noncardiac congenital anomalies. *Journal of Cardiac Surgery, 28(5),* 580–586. DOI 10.1111/jocs.12202.

2. Zhang, Y., Yang, Z. G., Yang, M. X., Shi, K., Li, R. et al. (2018). Common atrium and the associated malformations: Evaluation by low-dose dual-source computed tomography. *Medicine, 97(46),* e12983. DOI 10.1097/MD.0000000000012983.
3. Jacobs, J. P., Quintessenza, J. A., Burke, R. P., Mavroudis, C. (2000). Congenital heart surgery nomenclature and database project: Atrial septal defect. *The Annals of Thoracic Surgery, 69(3),* 18–24.
4. Khairy, P., Poirier, N., Mercier, L. A. (2007). Univentricular heart. *Circulation, 115(6),* 800–812. DOI 10.1161/CIRCULATIONAHA.105.592378.
5. Yang, M. X., Yang, Z. G., Zhang, Y., Shi, K., Xu, H. Y. et al. (2017). Dual-source computed tomography for evaluating pulmonary artery and aorta in pediatric patients with single ventricle. *Scientific Reports, 7(1),* 13398. DOI 10.1038/s41598-017-11809-6.
6. Watkins, W. S., Hernandez, E. J., Wesolowski, S., Bisgrove, B. W., Sunderland, R. T. et al. (2019). De novo and recessive forms of congenital heart disease have distinct genetic and phenotypic landscapes. *Nature Communications, 10(1),* 4722. DOI 10.1038/s41467-019-12582-y.
7. Hayabuchi, Y., Mori, K., Kitagawa, T., Inoue, M., Kagami, S. (2007). Accurate quantification of pulmonary artery diameter in patients with cyanotic congenital heart disease using multidetector-row computed tomography. *American Heart Journal, 154(4),* 783–788. DOI 10.1016/j.ahj.2007.06.004.
8. Ang, R., Hunter, R. J., Baker, V., Richmond, L., Dhinoja, M. et al. (2015). Pulmonary vein measurements on pre-procedural CT/MR imaging can predict difficult pulmonary vein isolation and phrenic nerve injury during cryoballoon ablation for paroxysmal atrial fibrillation. *International Journal of Cardiology, 195,* 253–258. DOI 10.1016/j.ijcard.2015.05.089.
9. Babu-Narayan, S. V., Giannakoulas, G., Valente, A. M., Li, W., Gatzoulis, M. A. (2016). Imaging of congenital heart disease in adults. *European Heart Journal, 37(15),* 1182–1195. DOI 10.1093/eurheartj/ehv519.
10. Shi, K., Yang, Z. G., Xu, H. Y., Zhao, S. X., Liu, X. et al. (2016). Dual-source computed tomography for evaluating pulmonary artery in pediatric patients with cyanotic congenital heart disease: Comparison with transthoracic echocardiography. *European Journal of Radiology, 85(1),* 187–192. DOI 10.1016/j.ejrad.2015.11.002.
11. Shi, K., Yang, Z. G., Chen, J., Zhang, G., Xu, H. Y. et al. (2015). Assessment of double outlet right ventricle associated with multiple malformations in pediatric patients using retrospective ECG-gated dual-source computed tomography. *PLoS One, 10(6),* e0130987. DOI 10.1371/journal.pone.0130987.
12. Hu, B. Y., Shi, K., Deng, Y. P., Diao, K. Y., Xu, H. Y. et al. (2017). Assessment of tetralogy of Fallot-associated congenital extracardiac vascular anomalies in pediatric patients using low-dose dual-source computed tomography. *BMC Cardiovascular Disorders, 17(1),* 285. DOI 10.1186/s12872-017-0718-8.
13. Dillman, J. R., Hernandez, R. J. (2009). Role of CT in the evaluation of congenital cardiovascular disease in children. *American Journal of Roentgenology, 192(5),* 1219–1231. DOI 10.2214/AJR.09.2382.
14. Gao, Y., Lu, B., Hou, Z., Yu, F., Cao, H. et al. (2012). Low dose dual-source CT angiography in infants with complex congenital heart disease: A randomized study. *European Journal of Radiology, 81(7),* e789–e795. DOI 10.1016/j.ejrad.2012.03.023.
15. Nie, P., Yang, G., Wang, X., Duan, Y., Xu, W. et al. (2014). Application of prospective ECG-gated high-pitch 128-slice dual-source CT angiography in the diagnosis of congenital extracardiac vascular anomalies in infants and children. *PLoS One, 9(12),* e115793. DOI 10.1371/journal.pone.0115793.
16. Lai, W. W., Geva, T., Shirali, G. S., Frommelt, P. C., Humes, R. A. et al. (2006). Guidelines and standards for performance of a pediatric echocardiogram: A report from the task force of the pediatric council of the american society of echocardiography. *Journal of the American Society of Echocardiography, 19(12),* 1413–1430. DOI 10.1016/j.echo.2006.09.001.
17. Kansy, A., Brzezinska-Rajszys, G., Zubrzycka, M., Mirkowicz-Malek, M., Maruszewski, P. et al. (2013). Pulmonary artery growth in univentricular physiology patients. *Kardiologia Polska, 71(6),* 581–587. DOI 10.5603/KP.2013.0121.
18. Yin, L., Lu, B., Han, L., Wu, R. Z., Johnson, L. et al. (2011). Quantitative analysis of pulmonary artery and pulmonary collaterals in preoperative patients with pulmonary artery atresia using dual-source computed tomography. *European Journal of Radiology, 79(3),* 480–485. DOI 10.1016/j.ejrad.2010.04.032.

19. Schwartzman, D., Lacomis, J., Wigginton, W. G. (2003). Characterization of left atrium and distal pulmonary vein morphology using multidimensional computed tomography. *Journal of the American College of Cardiology, 41(8),* 1349–1357. DOI 10.1016/S0735-1097(03)00124-4.
20. Ferns, S. J., El Zein, C., Multani, K., Sajan, I., Subramanian, S. et al. (2013). Is additional pulsatile pulmonary blood flow beneficial to patients with bidirectional Glenn? *Journal of Thoracic and Cardiovascular Surgery, 145(2),* 451–454. DOI 10.1016/j.jtcvs.2012.11.027.
21. Davies, R. R., Pizarro, C. (2015). Decision-making for surgery in the management of patients with univentricular heart. *Frontier Pediatric, 3,* 61. DOI 10.3389/fped.2015.00061.
22. Chaosuwannakit, N., Makarawate, P. (2018). Diagnostic accuracy of low-dose dual-source cardiac computed tomography as compared to surgery in univentricular heart patients. *Journal of Cardiothoracic Surgery, 13(1),* 39. DOI 10.1186/s13019-018-0729-2.
23. Edwards, R. M., Reddy, G. P., Kicska, G. (2016). The functional single ventricle: How imaging guides treatment. *Clinical Imaging, 40(6),* 1146–1155. DOI 10.1016/j.clinimag.2016.08.003.
24. Groh, M. A., Meliones, J. N., Bove, E. L., Kirklin, J. W., Blackstone, E. H. et al. (1991). Repair of tetralogy of Fallot in infancy. Effect of pulmonary artery size on outcome. *Circulation, 84(5 Suppl),* 206–212.
25. Lenoir, M., Pontailler, M., Gaudin, R., Gerelli, S., Tamisier, D. et al. (2017). Outcomes of palliative right ventricle to pulmonary artery connection for pulmonary atresia with ventricular septal defect. *European Journal of Cardio-Thoracic Surgery, 52(3),* 590–598. DOI 10.1093/ejcts/ezx194.
26. Reddy, V. M., McElhinney, D. B., Amin, Z., Moore, P., Parry, A. J. et al. (2000). Early and intermediate outcomes after repair of pulmonary atresia with ventricular septal defect and major aortopulmonary collateral arteries: experience with 85 patients. *Circulation, 101(15),* 1826–1832. DOI 10.1161/01.CIR.101.15.1826.
27. Reddy, V. M., Petrossian, E., McElhinney, D. B., Moore, P., Teitel, D. F. et al. (1997). One-stage complete unifocalization in infants: When should the ventricular septal defect be closed? *Journal of Thoracic and Cardiovascular Surgery, 113(5),* 858–866. DOI 10.1016/S0022-5223(97)70258-7.
28. Kawahira, Y., Kishimoto, H., Kawata, H., Ikawa, S., Ueda, H. et al. (1997). Diameters of the pulmonary arteries and veins as an indicator of bilateral and unilateral pulmonary blood flow in patients with congenital heart disease. *Journal of Cardiac Surgery, 12(4),* 253–260. DOI 10.1111/j.1540-8191.1997.tb00136.x.
29. Kawahira, Y., Kishimoto, H., Kawata, H., Ikawa, S., Ueda, H. et al. (1999). New indicator for the Fontan operation: Diameters of the pulmonary veins in patients with univentricular heart. *Journal of Cardiac Surgery, 14(4),* 259–265. DOI 10.1111/j.1540-8191.1999.tb00990.x.
30. Nabati, M., Bagheri, B., Habibi, V. (2013). Coincidence of total anomalous pulmonary venous drainage to the superior vena cava, common atrium, and single ventricle: A very rare condition. *Echocardiography, 30(4),* E98–E101. DOI 10.1111/echo.12141.
31. Chandrashekhar, G., Sodhi, K. S., Saxena, A. K., Rohit, M. K., Khandelwal, N. (2012). Correlation of 64 row MDCT, echocardiography and cardiac catheterization angiography in assessment of pulmonary arterial anatomy in children with cyanotic congenital heart disease. *European Journal of Radiology, 81(12),* 4211–4217. DOI 10.1016/j.ejrad.2012.08.010.
32. Cook, S. C., Raman, S. V. (2007). Unique application of multislice computed tomography in adults with congenital heart disease. *Internationl Journal of Cardiology, 119(1),* 101–106. DOI 10.1016/j.ijcard.2006.07.074.
33. Johnson, J. N., Hornik, C. P., Li, J. S., Benjamin, D. K., Jr., Yoshizumi, T. T. et al. (2014). Cumulative radiation exposure and cancer risk estimation in children with heart disease. *Circulation, 130(2),* 161–167. DOI 10.1161/CIRCULATIONAHA.113.005425.
34. Beausejour Ladouceur, V., Lawler, P. R., Gurvitz, M., Pilote, L., Eisenberg, M. J. et al. (2016). Exposure to low-dose ionizing radiation from cardiac procedures in patients with congenital heart disease: 15-year data from a population-based longitudinal cohort. *Circulation, 133(1),* 12–20. DOI 10.1161/CIRCULATIONAHA.115.019137.
35. Coles, D. R., Smail, M. A., Negus, I. S., Wilde, P., Oberhoff, M. et al. (2006). Comparison of radiation doses from multislice computed tomography coronary angiography and conventional diagnostic angiography. *Journal of the American College of Cardiology, 47(9),* 1840–1845. DOI 10.1016/j.jacc.2005.11.078.